Science Translational Medicine
AAAS

stm.sciencemag.org/cgi/content/full/11/513/eaax9364/DC1

Supplementary Materials for

An innate-like Vδ1$^+$ γδ T cell compartment in the human breast is associated with remission in triple-negative breast cancer

Yin Wu, Fernanda Kyle-Cezar, Richard T. Woolf, Cristina Naceur-Lombardelli, Julie Owen, Dhruva Biswas, Anna Lorenc, Pierre Vantourout, Patrycja Gazinska, Anita Grigoriadis, Andrew Tutt, Adrian Hayday*

*Corresponding author. Email: adrian.hayday@kcl.ac.uk

Published 9 October 2019, *Sci. Transl. Med.* **11**, eaax9364 (2019)
DOI: 10.1126/scitranslmed.aax9364

The PDF file includes:

Other Supplementary Material for this manuscript includes the following:

(available at stm.sciencemag.org/cgi/content/full/11/513/eaax9364/DC1)

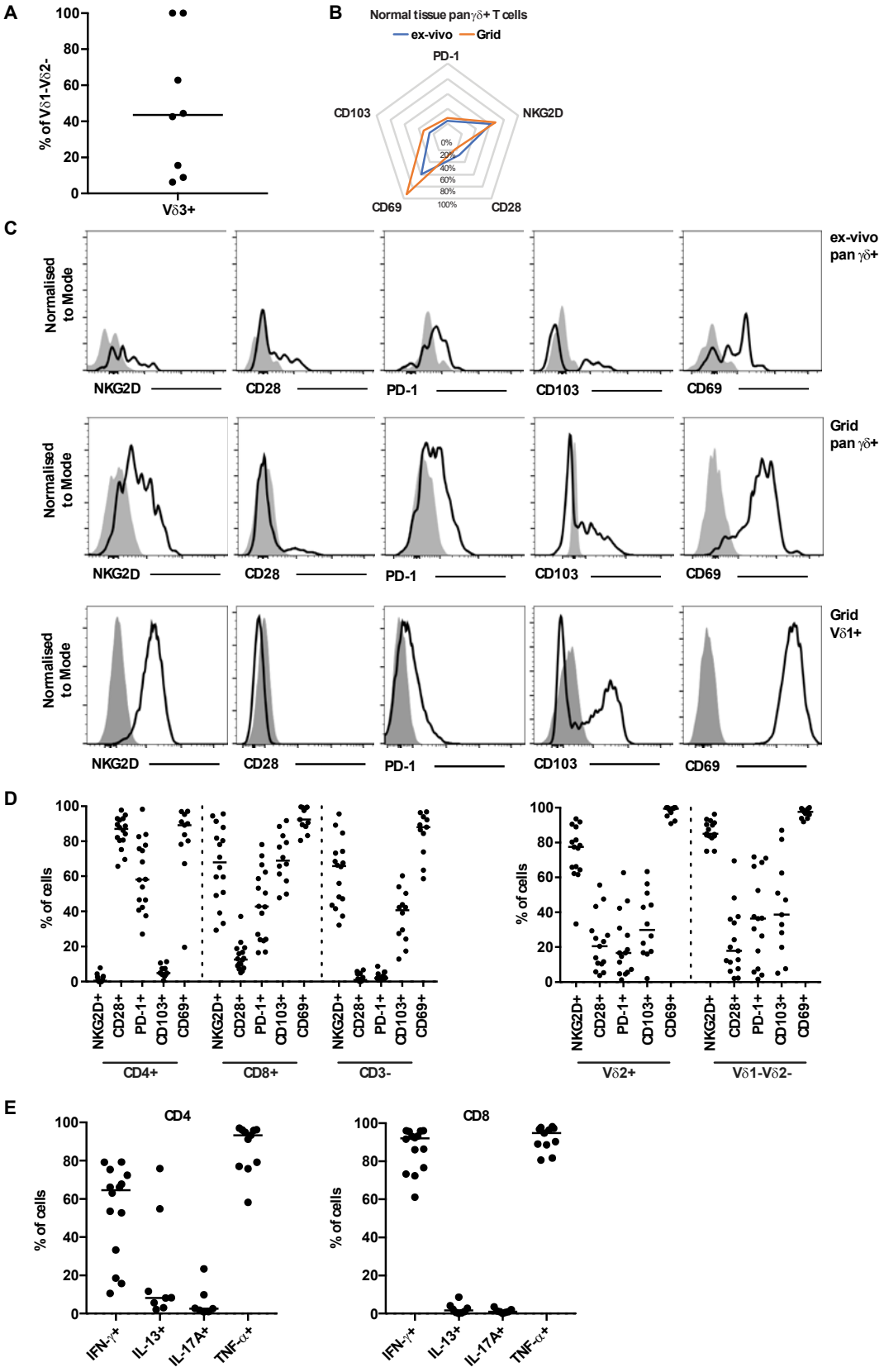
A
% of Vδ1-Vδ2-
Vδ3+
B
Normal tissue pan γδ+ T cells
ex-vivo
Grid
PD-1
NKG2D
CD28
CD69
CD103
C
Normalised to Mode
NKG2D
CD28
PD-1
CD103
CD69
ex-vivo pan γδ+
Grid pan γδ+
Grid Vδ1+
D
% of cells
NKG2D+
CD28+
PD-1+
CD103+
CD69+
CD4+
CD8+
CD3-
Vδ2+
Vδ1-Vδ2-
E
CD4
CD8
IFN-γ+
IL-13+
IL-17A+
TNF-α+

Fig. S1. Explant culture permitted the isolation of substantial numbers of human tissue-resident lymphocytes. **(A)** Scatter plot showing $V\delta3^+$ T cells as a percentage of $CD3^+\gamma\delta^+V\delta1^-V\delta2^-$ T cells. Median indicated. **(B)** Radar plot of surface marker expression on $\gamma\delta^+$ T cells directly isolated from normal breast tissue by dissociation (ex vivo) or via grid explant method from the same tissue (Grid). Mean plotted (n=3 for CD69; n=5 for CD28, CD103; n=6 for NKG2D, PD-1). **(C)** Representative histograms demonstrating expression of the cell surface markers NKG2D, CD28, PD-1, CD103 and CD69 on ex vivo isolated pan γδ T cells (upper panel), grid isolated pan γδ T cells (middle panel) and grid isolated $V\delta1^+$ T cells (bottom panel). **(D)** Scatter plots showing breast-resident lymphocyte expression of the surface markers NKG2D (n=14-16 depending on cell type), CD28 (n=14-16 depending on cell type), PD-1 (n=14-16 depending on cell type), CD103 (n=11-12 depending on cell type), and CD69 (n=11). Median indicated. **(E)** Tissue-resident αβ T cells cytokine-production profiles. Scatter plots showing intracellular cytokine staining of breast-resident $CD4^+$ and $CD8^+$ αβ T cells for IFN-γ (n=14), IL-13 (n=8), IL-17A (n=7) and TNF-α (n=11) following *in vitro* activation with PMA (10 ng/ml) and ionomycin (1 μg/ml) with BFA (20 μg/ml) [4h]. Median indicated.

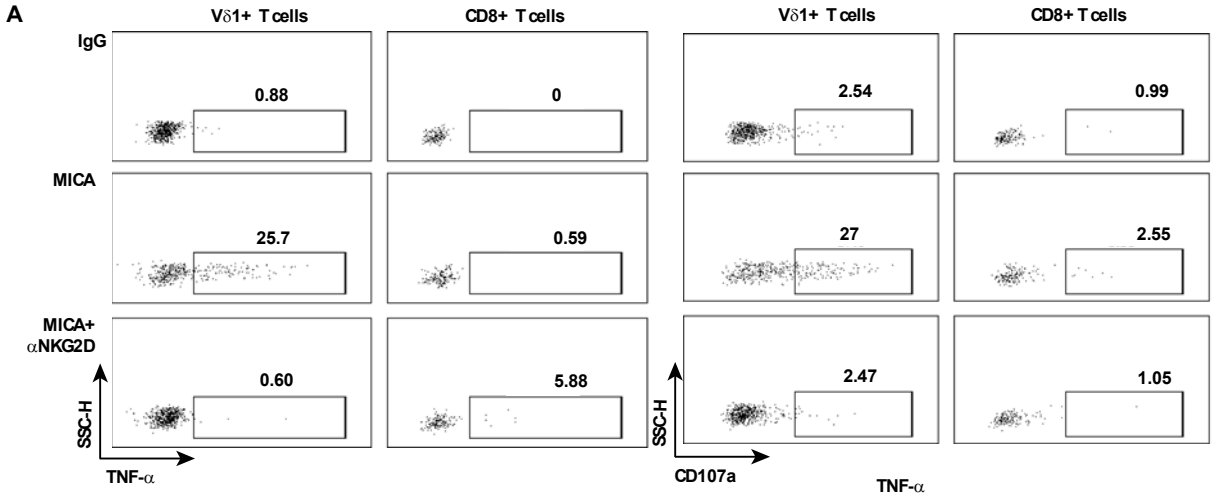
A
Vδ1+ Tcells
CD8+ Tcells
Vδ1+ Tcells
CD8+ Tcells
IgG
0.88
0
2.54
0.99
MICA
25.7
0.59
27
2.55
MICA+ αNKG2D
0.60
5.88
2.47
1.05
SSC-H
TNF-α
SSC-H
CD107a
TNF-α

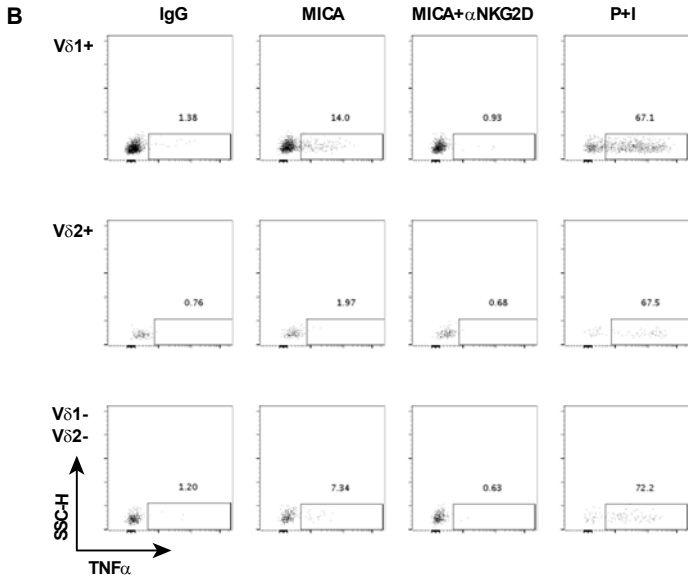
B
IgG
MICA
MICA+αNKG2D
P+I
Vδ1+
1.38
14.0
0.93
67.1
Vδ2+
0.76
1.97
0.68
67.5
Vδ1-
Vδ2-
1.20
7.34
0.63
72.2
SSC-H
TNFα
IgG
MICA
MICA+αNKG2D
P+I
Vδ1+
6.64
36.5
7.31
89.6
Vδ2+
2.29
7.24
10.3
100
Vδ1-
Vδ2-
3.92
19.9
8.15
77.8
SSC-H
CD107a

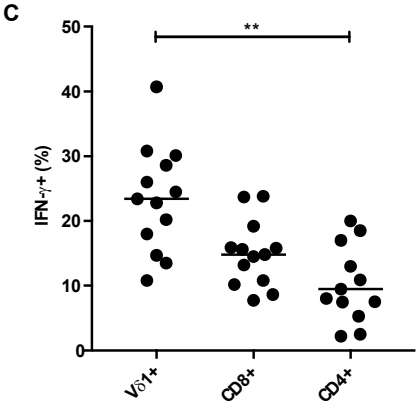
C
**
IFN-γ+ (%)
50
40
30
20
10
0
Vδ1+
CD8+
CD4+

Fig. S2. Vδ1^{+} T cells display innate-like responsiveness. (A) Representative dot plots showing intracellular staining for TNF-α and CD107a following *in vitro* activation of breast tissue-derived T cells with negative control plate-bound IgG (10 μg/ml), recombinant MICA (10 μg/ml) and recombinant MICA + blocking anti-human NKG2D antibody (10 μg/ml) in presence of BFA (20 μg/ml) [6h]. **(B)** Representative dot plots for two donors showing intracellular staining for TNF-α and CD107a following *in vitro* activation as described above, and also with PMA/ionomycin (P+I). **(C)** Scatter plot showing intracellular IFN-γ production following *in vitro* activation of breast-resident lymphocytes with IL-12 (100 ng/ml) and IL-18 (100 ng/ml) over 24-hours in the presence of BFA (20 μg/ml) for the last 4 hours (n=13); median indicated. *p<0.05, **p≤0.01, ***p≤0.001, ****p≤0.0001, Kruskal-Wallis with *post-hoc* Dunn's test corrected for multiple testing.

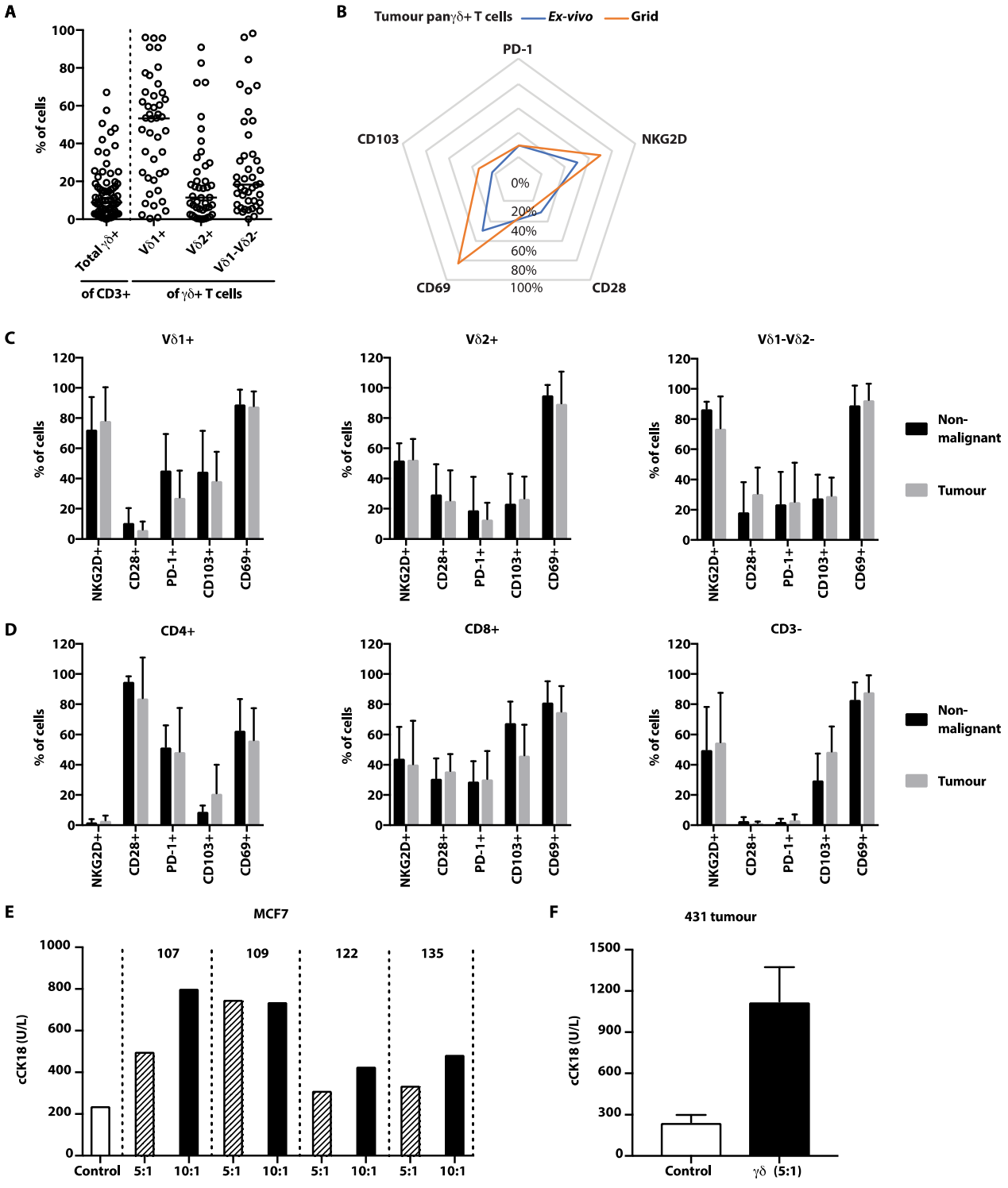

Fig. S3. αβ and γδ T cells isolated from breast tumors phenotypically resemble those from healthy tissue.

(A) γδ T cells were consistently isolated from human breast tumor samples. Scatter plots showing the number of γδ TCR$^+$ cells isolated from tumor expressed as a percentage of CD3$^+$ cells (n=79), with the proportion of Vδ1$^+$, Vδ2$^+$

and Vδ1^{-}Vδ2^{-} cell subsets shown (n=44); median indicated. **(B)** Radar plot of surface marker expression on γδ^{+} T cells directly isolated from breast tumor tissue by dissociation (ex vivo) or via grid explant method from the same tumor (Grid). Mean value plotted (n=5 for CD69; n=6 for CD103, CD28, NKG2D, PD-1). **(C)** Surface markers of breast tumor-resident γδ T cells (gray) compared with healthy breast tissue-resident γδ T cells (black). NKG2D (n=4-6 depending on Vδ subset), CD28 (n=4-6 depending on Vδ subset), PD-1 (n=4-6 depending on Vδ subset), CD103 (n=5-11 depending on Vδ subset) and CD69 (n=5-11 depending on Vδ subset); mean with SEM indicated. **(D)** Surface markers of other tumor-resident lymphocyte subsets. n=9 paired samples; mean with SEM indicated. **(E)** Breast tissue-resident γδ T cell killing of a tumor cell line. Negatively-sorted tissue derived effector γδ T cells from four healthy donors (107, 109, 122, and 135) were incubated with target MCF7 tumor cell line at 5:1 and 10:1 effector:target ratios. Target cells alone were used as control for background cell death (Control). Tumor cell line killing was measured by caspase-cleaved cytokeratin 18 (cCK18). **(F)** Breast tumor-resident γδ T cell killing of autologous tumor cells. Negatively-sorted tumor derived effector γδ T cells from patient 431 were incubated with autologous tumor cells at a 5:1 effector:target ratio. Target cells alone were used a control for background cell death (Control). Autologous tumor cell killing was measured by caspase-cleaved cytokeratin 18 (cCK18); mean of two technical replicates plotted ± SEM.

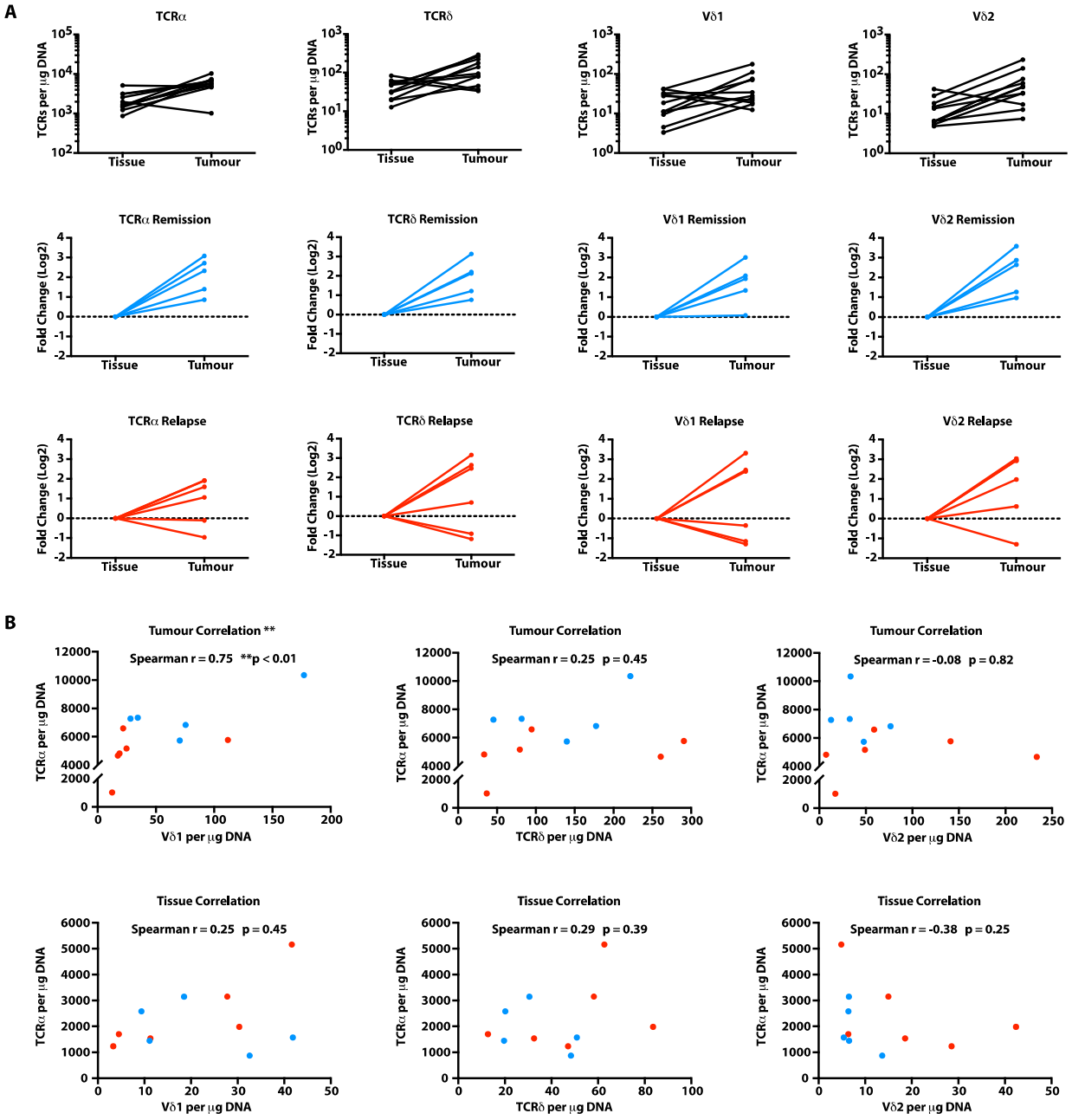

Fig. S4. Both αβ and γδ T cells are enriched in tumors compared with paired non-malignant tissue. (A) Absolute TCR copies (T cell numbers) are plotted per microgram of input DNA and paired between non-malignant tissue ("Tissue") and matched tumor tissue ("Tumor") for αβ T cells (TCRα), for total γδ T cells (TCRδ), Vδ1 T cells and Vδ2 T cells. Subjects were split by remission (blue) versus relapse (red) and expressed as fold change relative to paired tissue counts. **(B)** Absolute TCRα copies (αβ T cells) are plotted against total TCRδ (γδ T cells),

Vδ1 and Vδ2 copies per microgram of input DNA from tumor tissue (“Tumor”) and non-malignant tissue (“Tissue”). Correlations were determined by Spearman test.

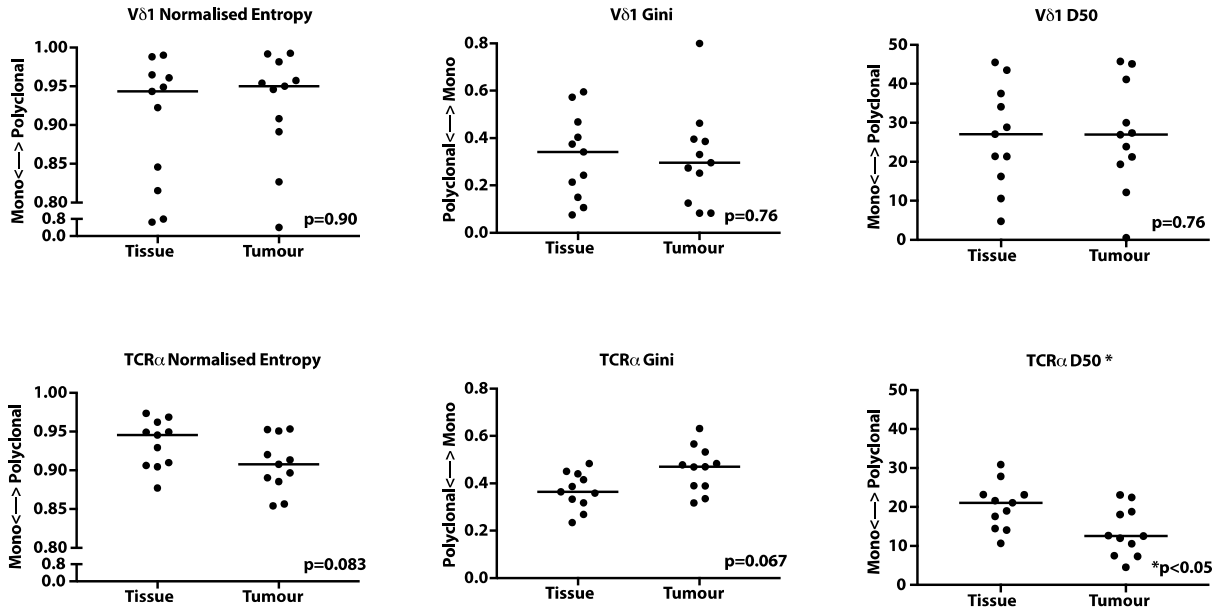

Fig. S5. Vδ1^{+} T cells show no evidence of tumoral clonal focusing in contrast to αβ T cells. Repertoire metrics applied to raw, non-downsampled (raw) TCRs, using normalised measures of clonality (Normalised entropy, Gini coefficient, D50). Wilcoxon matched pairs signed rank test was used to compare tumor to non-malignant tissue TCR diversity, *p<0.05, n=11pairs. All sequences were analysed based on amino acid sequence; median bar plotted.

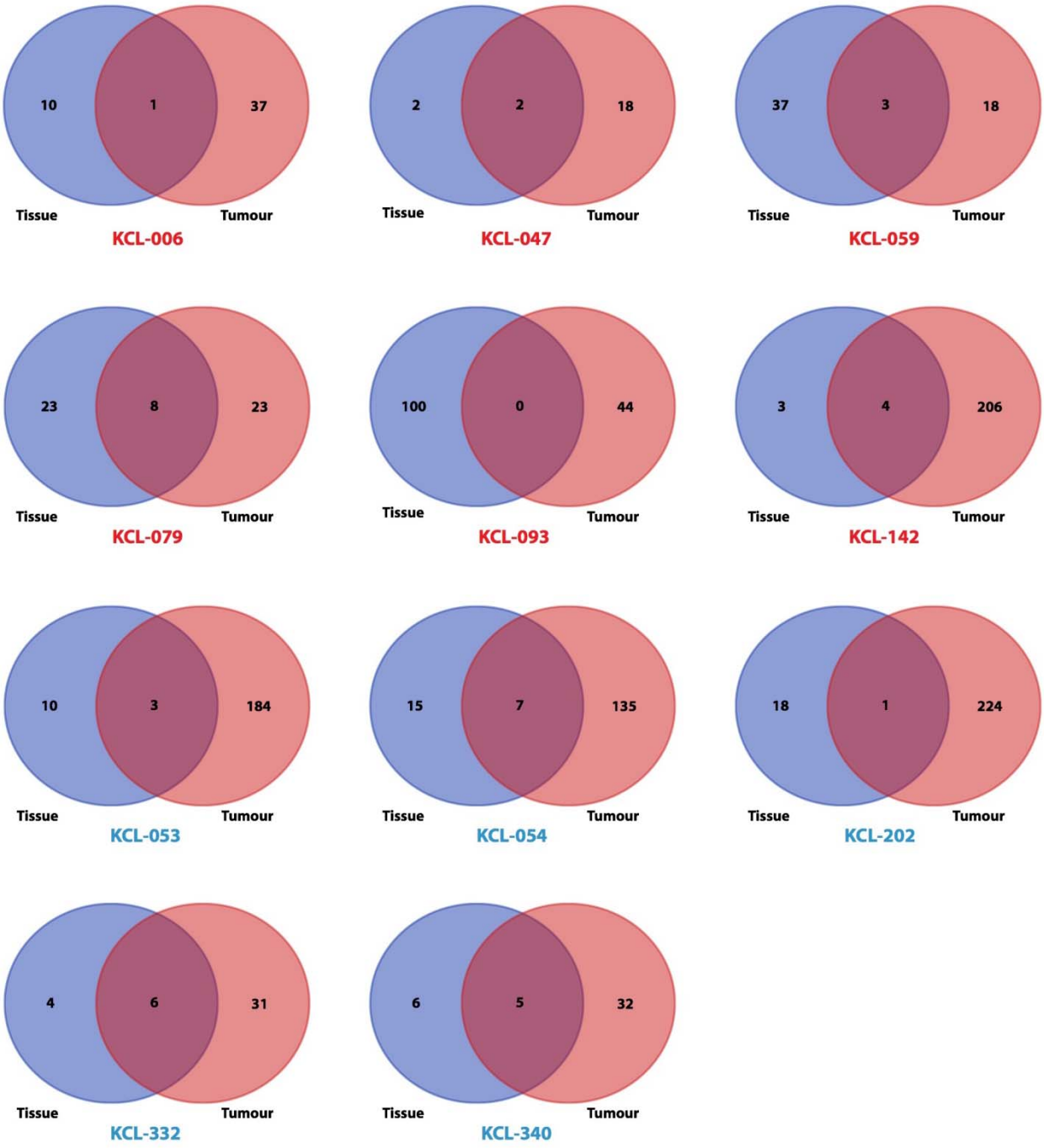

Fig. S6. There is limited Vδ1 repertoire overlap between tumor and paired non-malignant tissue within patients. Venn diagrams showing Vδ1^{+} clonotypes found in non-malignant tissue ("Tissue" - blue shade) and paired tumor tissue ("Tumor" - red shade), and clonotypes shared between the two (intersection). All sequences were analysed based on amino acid sequence.

Table S1. Lymphocyte subtypes observed ex vivo after enzymatic digestion and in grid explant cultures. Summary data comparing cells directly ex vivo with grid explants for $CD3^+$ cells and $CD3^-CD56^+$ cells, each expressed as proportions of $CD45^+$ cells, and $CD4^+$, $CD8^+$ and $TCR\gamma\delta^+$ cells each expressed as percentages of $CD45^+$ $CD3^+$ cells. Number of samples indicated *(n)*, mean ± SD reported.

		Non-malignant Tissue		**Breast tumor**	
		ex vivo	**Grid**	**ex vivo**	**Grid**
% CD45+	**CD3+**	**86.5 ± 10.14**	**86.1 ± 11.7**	**82.7 ± 7.1**	**83.6 ± 13.1**
	(n)	*(10)*	*(70)*	*(26)*	*(69)*
	CD3-CD56+	**1.2 ± 1.3**	**8.6 ± 8.8**	**4.5 ± 4.6**	**13.7 ± 12.2**
	(n)	*(10)*	*(43)*	*(26)*	*(40)*
% CD45+CD3+	**CD8+**	**42.5 ± 16.9**	**41.9 ± 20.6**	**32.4 ± 9.5**	**41.9 ± 24.3**
	(n)	*(10)*	*(70)*	*(26)*	*(69)*
	CD4+	**47.2 ± 17.7**	**52.2 ± 21.6**	**52.2 ± 21.6**	**53.6 ± 27.2**
	(n)	*(10)*	*(70)*	*(26)*	*(69)*
	γδ+	**3.1 ± 4.1**	**6.5 ± 8.5**	**2.9 ± 2.6**	**12.5 ± 12.3**
	(n)	*(10)*	*(70)*	*(26)*	*(69)*

Table S2. Clinical features of KCL TNBC cohort. Age: age in years at diagnosis. Stage: Tumor-node-metastasis (TNM) stage at diagnosis. Treatment: adjuvant/neoadjuvant regimen, not including subsequent salvage treatments at relapse (FEC-T: Fluorouracil, epirubicin, cyclophosphamide and docetaxel, TC: docetaxel, cyclophosphamide, EC-T: epirubicin, cyclophosphamide and docetaxel, T-EC: docetaxel and epirubicin, cyclophosphamide). PFS: progression free survival in months. OS: overall survival in months.

Patient ID	Age	Stage	Treatment	Relapse site	Biopsy Proven	PFS	OS
KCL-006	31	IA (T1cN0)	FEC-T	Axilla	Yes	7.77	42.50
KCL-047	72	IIIC (T2N3a)	Declined chemotherapy	Chest wall and axilla	Yes	6.73	12.50
KCL-053	49	IA (T1cN0)	TC	N/A	N/A	61.40	61.40
KCL-054	53	IIA (T2N0)	Weekly paclitaxel	N/A	N/A	62.60	62.60
KCL-059	38	IIB (T3N0)	EC-T	Brain metastasis	No – (radiological – MRI)	12.87	26.90
KCL-079	61	IIA (T2N0)	T-EC	Axilla	Yes	17.27	35.13
KCL-093	48	IIB (T3N0)	T-EC	Lung	Yes	10.73	20.40
KCL-142	38	IIB (T2N1a)	FEC-weekly paclitaxel	Chest wall	Yes	11.47	28.07
KCL-202	40	IIA (T2N0)	TC	N/A	N/A	55.73	55.73
KCL-332	75	IIA (T2N0)	Declined chemotherapy	N/A	N/A	48.07	48.07
KCL-340	87	IIIA (T3N1)	Not fit for chemotherapy	N/A	N/A	51.10	51.10

Table S3. Clonality metrics of downsampled TCRs. Gini Coefficient (0=polyclonal, 1=monoclonal)**,** D50 (0=monoclonal, 50=polyclonal).

TCR Locus	Patient ID	Gini Coefficient		D50	
		Tissue	Tumor	*Tissue*	Tumor
TCRδ (down sampled)	KCL-006	*0.229*	0.133	*42.9*	50.0
	KCL-047	*0.150*	0.142	*50.0*	50.0
	KCL-053	*0.289*	0.050	*33.3*	50.0
	KCL-054	*0.558*	0.706	*15.8*	3.4
	KCL-059	*0.259*	0.317	*31.8*	30.1
	KCL-079	*0.364*	0.415	*27.3*	23.1
	KCL-093	*0.182*	0.281	*35.9*	31.0
	KCL-142	*0.353*	0.055	*40.0*	50.0
	KCL-202	*0.608*	0.101	*8.3*	45.8
	KCL-332	*0.452*	0.260	*25.0*	31.8
	KCL-340	*0.275*	0.300	*37.5*	30.0
TCRα (Top 10% down sampled)	KCL-006	*0.606*	0.610	*0.85*	0.75
	KCL-047	*0.540*	0.632	*1.13*	0.65
	KCL-053	*0.381*	0.508	*2.38*	1.51
	KCL-054	*0.335*	0.582	*2.64*	0.93
	KCL-059	*0.513*	0.380	*1.42*	2.36
	KCL-079	*0.428*	0.550	*1.96*	1.18
	KCL-093	*0.571*	0.597	*0.98*	0.86
	KCL-142	*0.462*	0.579	*1.70*	0.97
	KCL-202	*0.534*	0.426	*1.16*	2.07
	KCL-332	*0.342*	0.399	*2.71*	2.08
	KCL-340	*0.420*	0.528	*2.02*	1.35

Table S4. Clonality metrics of raw TCRs. Normalized Shannon Entropy (0=monoclonal, 1=polyclonal). Gini Coefficient (0=polyclonal, 1=monoclonal). D50 (0=monoclonal, 50=polyclonal)

TCR Locus	Patient ID	Normalized Shannon Entropy		Gini Coefficient		D50	
		Tissue	Tumor	*Tissue*	Tumor	*Tissue*	Tumor
TCRδ (Raw)	KCL-006	*0.988*	0.954	*0.076*	0.296	*45.5*	27.0
	KCL-047	*0.961*	0.908	*0.150*	0.396	*37.5*	21.3
	KCL-053	*0.949*	0.992	*0.243*	0.083	*28.8*	45.7
	KCL-054	*0.797*	0.408	*0.573*	0.800	*10.6*	0.5
	KCL-059	*0.943*	0.950	*0.341*	0.274	*27.1*	27.4
	KCL-079	*0.922*	0.891	*0.375*	0.386	*21.4*	19.4
	KCL-093	*0.990*	0.982	*0.106*	0.125	*43.5*	41.1
	KCL-142	*0.846*	0.957	*0.403*	0.252	*21.4*	30.0
	KCL-202	*0.649*	0.993	*0.595*	0.083	*4.7*	45.1
	KCL-332	*0.815*	0.946	*0.468*	0.330	*16.3*	23.9
	KCL-340	*0.965*	0.827	*0.214*	0.463	*34.1*	12.2
TCRα (Raw)	KCL-006	*0.877*	0.908	*0.483*	0.390	*10.6*	18.1
	KCL-047	*0.906*	0.854	*0.415*	0.533	*17.6*	7.5
	KCL-053	*0.969*	0.953	*0.268*	0.317	*27.8*	23.1
	KCL-054	*0.962*	0.857	*0.333*	0.631	*23.2*	4.5
	KCL-059	*0.929*	0.953	*0.387*	0.335	*19.0*	22.4
	KCL-079	*0.949*	0.914	*0.359*	0.470	*21.1*	12.6
	KCL-093	*0.910*	0.890	*0.451*	0.483	*14.1*	10.6
	KCL-142	*0.950*	0.897	*0.318*	0.470	*23.1*	12.0
	KCL-202	*0.905*	0.951	*0.440*	0.390	*14.5*	18.8
	KCL-332	*0.973*	0.920	*0.235*	0.478	*30.9*	12.5
	KCL-340	*0.945*	0.885	*0.364*	0.566	*21.6*	7.3

Table S5. Public intratumoral phospho-antigen reactive Vδ2 CDR3 sequences and samples in which they were shared. All shared CDR3s had a conserved hydrophobic residue in position 97 (denoted in bold).

Vδ2 CDR3 (amino acid sequence)	Present in
CACDT**L**GDTDKLIF	KCL-059, KCL-079, KCL-142
CACDA**L**LGDTDKLIF	KCL-053, KCL-059, KCL -142
CACDT**V**GGYTDKLIF	KCL-054, KCL-340

Table S6. Antibodies and key reagents table.

Antibodies		
Anti-human CD103 PE	BioLegend	Cat. number: 350206
Anti-human CD107a PE	BioLegend	Cat. number: 328608
Anti-human CD279 (PD-1) APC/Cy7	BioLegend	Cat. number: 329922
Anti-human CD28 PE	BioLegend	Cat. number: 302908
Anti-human CD3 BUV 395	BD Biosciences	Cat. number: 563546
Anti-human CD3 APC	BioLegend	Cat. number: 317318
Anti-human CD314 (NKG2D) APC	BioLegend	Cat. number: 320808
Anti-human CD335 (NKp46) PerCP/Cy5.5	BioLegend	Cat. number: 331920
Anti-human CD4 Brilliant Violet 785	BioLegend	Cat. number: 300554
Anti-human CD45 Brilliant Violet 605	BioLegend	Cat. number: 304042
Anti-human CD56 Pacific Blue	BioLegend	Cat. number: 304629
Anti-human CD69 Alexa Fluor 700	BioLegend	Cat. number: 310922
Anti-human CD8a Brilliant Violet 785	BioLegend	Cat. number: 301046
Anti-human CD8a APC/Cy7	BioLegend	Cat. number: 301016
Anti-human TCRab PE	BioLegend	Cat. number: 306708
Anti-human TCRgd PE/Cy7	Beckman Coulter	Cat. number: B10247
Anti-human TCR Vδ1 FITC	Thermo Fisher Scientific	Cat. number: TCR2730
Anti-human TCR Vδ2 PerCP	BioLegend	Cat. number: 331410
Anti-human TCR Vδ3 APC	Beckman Coulter	Cat. number: IM99513
Anti-human IFNγ Brilliant Violet 421	BioLegend	Cat. number: 502532
Anti-human IL13 PE	BioLegend	Cat. number: 501903
Anti-human IL17A Alexa Fluor 647	BioLegend	Cat. number: 512309
Anti-human TNFα APC	BioLegend	Cat. number: 502913
Mouse Isotype Control IgG1, k Alexa Fluor 647	BioLegend	Cat. number: 400136
Mouse Isotype Control IgG1, k APC	BioLegend	Cat. number: 400122
Mouse Isotype Control IgG1, k PE	BioLegend	Cat. number: 400113
Mouse Isotype Control IgG1, k PerCP/Cy5.5	BioLegend	Cat. number: 400150
Mouse Isotype Control IgG2b, k PE	BioLegend	Cat. number: 401208
Anti-human CD3	BioLegend	Cat. number: 317326
Anti-human CD314 (NKG2D)	BioLegend	Cat. number: 320810
Purified mouse IgG2, κ	BioLegend	Cat. number: 400223
Chemicals, Peptides, and Recombinant Proteins		
Monensin Solution (1000x)	BioLegend	Cat. number: 420701
Recombinant MICA-Fc chimera	R&D Systems	Cat. number: 1300-MA-050
Recombinant Human IL-1β	BioLegend	Cat. number: 579402
Recombinant Human IL-2 (Proleukin)	Novartis	Cat. number: N/A
Recombinant Human IL-6	BioLegend	Cat. number: 570802

Recombinant Human IL-15	BioLegend	Cat. number: 570308
Recombinant Human IL-23	BioLegend	Cat. number: 574102
Recombinant Human TGF-β1	BioLegend	Cat. number: 580702
Commercial Kits		
M30 CytoDEATH CK18 Kit	Diapharma	Cat. Number: P10900
MACS Human Tumor Dissociation Kit	Miltenyi Biotec	Cat. Number: 130-095-929
QIAamp DNA FFPE Tissue Kit	Qiagen	Cat. Number: 56404
Software and Algorithms		
immunoSEQ Analyzer	https://clients.adaptivebiotech.com/login	
MacroFocus Treemap	https://www.treemap.com	
UpSet R package	https://vcg.github.io/upset	
TCR sequence repository	https://osf.io/d4eu6	
Prism 7	GraphPad	